Elsevier Editorial System(tm) for Surface and Coatings Technology

Manuscript Draft

Manuscript Number: SURFCOAT-D-15-01941R2

Title: Surface texturing of Si3N4-SiC ceramic tool components by pulsed laser machining

Article Type: Full Length Article

Keywords: silicon nitride; pulsed laser machining; surface texturing; material removal; roughness

Corresponding Author: Mrs. Lerato Criscelda Tshabalala, MTech

Corresponding Author's Institution: Tshwane University of Technology

First Author: Sisa L Pityana, PhD

Order of Authors: Sisa L Pityana, PhD; Lerato Criscelda Tshabalala, MTech

Abstract: Traditional abrasive techniques such as grinding and lapping have long been used in the surface conditioning of engineering materials. However, in the processing of hard and brittle materials like Silicon Nitride (Si3N4), machining is often accompanied by numerous shortcomings which either lead to poor surface quality or residual surface damage of the workpiece. In this sense, this work focuses on the application of a pulsed mode, nanosecond Nd:YAG laser system for the surface texturing of Si3N4-SiC composites in the fabrication of machining tool inserts for various tribological applications. The samples were machined at varied laser energy (0.1-0.6 mJ) and lateral pulse overlap (50-88%) in order to generate a sequence of linear parallel micro-grooves on the sample surfaces. The results showed a logarithmic increase in material removal as pulse energy and lateral overlaps were increased. The material removal threshold was established at 0.1mJ (0.80x105 J/m2). Optimum surface texturing was achieved at a combination of 0.3 mJ (2.38x105 J/m2) and 50%, pulse energy and lateral pulse overlap respectively.

***Cover Letter**

L.C. Tshabalala
Tshwane University of Technology
Department of Chemical, Metallurgical & Materials Engineering, Pretoria West Campus, Room 2-152, Pretoria 0001, South Africa
tshabalalalc@tut.ac.za
November 19, 2015

To the Editor
Journal of Surface & Coatings Technology

Dear Editor

I am pleased to submit an original research article titled "Surface texturing of Si_3N_4-SiC ceramic tool components by pulsed laser machining " by L.C. Tshabalala (*corresponding author*) and S.L. Pityana for consideration in the *Journal of Surface & Coatings Technology*. The main aim for this research is to investigate the application of pulsed laser systems in the machining/texturing of Silicon Nitride-based ceramics.

In this manuscript, we show the material response to various laser parameters (pulse energy and pulse overlap). For this article, we only focused on profiling the material removal depth, scan width, material removal rates and the surface roughness after using two dimensional (2D) and three dimensional (3D) machining procedures. In line with the process characterisation outputs of material removal depth (~10µm) and a final surface roughness of 1.5 µm ≤ Ra ≤ 2.5µm for 2D machining and 2.5 µm ≤ Sa ≤ 5µm for 3D machining, the results showed that surface texturing can be achieved using pulsed laser machining with careful control of the parameters as the objective were achieved. This work will form a basis for various future works in line with the commercialization of laser textured Silicon Nitride machining tools as it reports on the machining parameter optimization profiles.

This work has not been published and is not under consideration elsewhere. If you feel that the manuscript is appropriate for this journal, we have suggested the list of reviewers as included in the online submission (or see the next page). For more information, feel free to contact the corresponding author.

Thank you for your consideration.

Sincerely
Tshabalala L.C, M-Tech, Technologist
Tshwane University of Technology, Department of Chemical, Metallurgical & Martials Engineering

The list of suggested reviewers by the corresponding author:

First Name	Middle Initial	Last Name	Academic Degree	Institution	E-mail Address
Andrew		Dunn		Institute of Photonics and Quantum Sciences, Heriot-Watt University, Edinburgh, Scotland EH14 4AS, UK	ad134@hw.ac.uk
Narendra	B	Dahotre		Laboratory of Laser Materials Processing & Synthesis, Center for Advanced Research & Technology (CART), USA	Narendra.Dahotre@unt.edu
Luís	L	Vilhena		University of Ljubljana, Centre for Tribology and Technical Diagnostics, Bogisiceva 8, SLO 1000 Ljubljana, Slovenia	LVilhena@ctd.uni-lj.si

***Response to Reviewers**

L.C. Tshabalala
Tshwane University of Technology
Department of Chemical, Metallurgical &
Materials Engineering, Pretoria West Campus,
Room 2-152, Pretoria 0001, South Africa
tshabalalalc@tut.ac.za
November 19, 2015

To reviewers
Journal of Surface & Coatings Technology

Dear Reviewer

I am pleased to submit a second revision of the manuscript as per recommendations highlighted in the revision letter. The authors sincerely appreciate the expertise, time and dedication of the reviewers. Their guidance has been invaluable during this research. As per comments in the review letter, the following changes were made:

- INTRODUCTION: The references were used properly as recommended by the reviewer. The introduction was edited so as to direct the focus to the surface texturing of silicon nitride based ceramics by: (i) switching paragraph 2 with paragraph 3, (ii) additional statements were added to emphasize the properties of silicon nitride based ceramics.
- MATERIALS AND METHODS: Grammatical errors were checked and corrected as highlighted on the revised document. In Table 1, the material used was edited to "Si_3N_4-SiC (SL-506)", the colour of the samples was edited to "Light green".
- RESULTS AN DISCUSSION: Line 4 and the last paragraph were edited as per reviewer comments. Also, the changes in surface chemistry are explained in line with the chemical equations presented in Table 4. The equations 9 and 13 were edited.
- REFERENCES: The relevant sources were cited properly as per reviewer comments.

I believe that we have attended to the recommendations by the reviewers to our level best. Their expertise was highly appreciated. For more information, feel free to contact the corresponding author. Thank you for your consideration

Sincerely

Tshabalala L.C, M-Tech, Technologist
Tshwane University of Technology, Department of Chemical, Metallurgical & Martials Engineering
Tel: (+27) 12 382 4244, E-mail: tshabalalalc@tut.ac.za , ckgomari@yahoo.com

***Highlights (for review)**

HIGHLIGHTS

- Parallel laser scans were used to texture the surface of a Silicon Nitride-Silicon Carbide composite (Si_3N_4-SiC).
- Material removal rate increased logarithmically with the increasing pulse energy, 0.1-0.6 mJ and lateral pulse overlap, 50%, 75%, and 88%.
- Material removal threshold was established at ~0.1mJ ($0.80x10^5$ J/m^2) for the investigated pulse overlap settings.
- High surface roughness was obtained using the 88% pulse overlap regime.
- Better control of the laser texturing process was obtained within the 0.3mJ energy range and low lateral pulse overlap.
- Surface morphology and chemistry occurred by dissociation, melting and evaporation which lead to an increase in surface silicon, oxygen, aluminum and loss of nitrogen and carbon.

Surface texturing of Si_3N_4-SiC ceramic tool components by pulsed laser machining

Lerato Criscelda Tshabalala[1], Sisa Pityana[2]

[1]Department of Chemical, Metallurgical and Materials Engineering, Tshwane University of Technology, Pretoria West Campus, Room 2-152,Pretoria 0001, South Africa, e-mail: tshabalalalc@tut.ac.za

[2]Council for Scientific and Industrial Research (CSIR), National Laser Center, Building 46A, P.O. Box 395, Pretoria 0001, South Africa, e-mail: spityana@csir.co.za

[1]Corresponding author

Abstract: - Traditional abrasive techniques such as grinding and lapping have long been used in the surface conditioning of engineering materials. However, in the processing of hard and brittle materials like Silicon Nitride (Si_3N_4), machining is often accompanied by numerous shortcomings which either lead to poor surface quality or residual surface damage of the workpiece. In this sense, this work focuses on the application of a pulsed mode, nanosecond Nd:YAG laser system for the surface texturing of Si_3N_4-SiC composites in the fabrication of machining tool inserts for various tribological applications. The samples were machined at varied laser energy (0.1-0.6 mJ) and lateral pulse overlap (50-88%) in order to generate a sequence of linear parallel micro-grooves on the sample surfaces. The results showed a logarithmic increase in material removal as pulse energy and lateral overlaps were increased. The material removal threshold was established at 0.1mJ ($0.80x10^5$ J/m^2). Optimum surface texturing was achieved at a combination of 0.3 mJ ($2.38x10^5$ J/m^2) and 50%, pulse energy and lateral pulse overlap respectively.

Keywords: - Si_3N_4, Pulsed laser machining, Material removal

---

1. INTRODUCTION

Industrial applications of pulsed laser machining (PLM) as an alternative to traditional surface treatment techniques like milling, cutting, grinding and lapping have increased considerably in the recent decade [1-3]. The popularity of pulsed laser systems, particularly in the surface texturing of structural ceramics has been partly credited to their high precision, flexibility, repeatable and controllable material removal rates which can be attained with negligible effects on the properties of the bulk material [4-6]. These benefits have encouraged research and commercial interest in the fabrication of machining tools from hard to machine structural ceramics like alumina (Al_2O_3), silicon carbide (SiC), silicon nitride (Si_3N_4), and other engineering materials [1,7].

In accordance with this research, a pulsed laser system has been utilized in the surface texturing of Si_3N_4-SiC ceramic components for the fabrication of machining tools. Silicon nitride based ceramics have numerous superlative properties which make them appropriate for a wide range of engineering applications. For example, their chemical inertness makes them suitable for corrosive environments and skeletal implants in medical applications. Their low thermal conductivity and density, high hardness and toughness gives them high thermal stability and robustness which are prerequisites for machining tools, engine parts and crucibles [8]. However, the surface texturing of Si_3N_4 based ceramics by the aforementioned abrasive techniques has been reported to be rather difficult due to the inherently high fracture toughness and high hardness of these materials. As a result, some of the drawbacks associated with the abrasive texturing processes include low throughput, labour intensiveness and surface damage (surface flaws and machining marks). Also, the induced thermal and mechanical damage to the machining tools often leads to poor repeatability of the surface quality and additional operational costs. In addition, their restricted plasticity makes them brittle at ambient temperature. This causes them to rupture without appreciable plastic strain just after the applied tensile load exceeds their yield strength [8, 9]. In light of this, the initial motivation for this research has been the need for innovative and cost efficient surface treatment solutions that can allow for better control on quality (surface roughness) and lead to precise and repeatable material removal rates during the fabrication of complex three-dimensional (3D) structures.

Secondly, the challenges associated with the tribological applications of the ceramic tools constitute a secondary concern that can be addressed by this research. During service, machining is often affected by severe friction effects which include high surface temperatures and high wear rates, mainly due to the presence of

workpiece chips at the contact surfaces [10]. The effects of these conditions on tool life are often curbed by applying lubricants during machining. However, the use of lubricating fluids increases operational cost, creates negative environmental impacts and raises serious health issues [10]. Researchers have investigated alternative methods towards the reduction of consumption or the elimination of lubrication fluids in abrasive machining processes. Amongst the various proposed solutions, applications of minimum quantity lubrication (MQL) techniques and machining under dry and near dry machining conditions have been a subject of investigation by various researchers [10-15].

Recently, researchers have also demonstrated surface texturing as an effective method of improving the tribological performance of machining tools [15-21]. Texturing entails the generation of imperfections on the surface of a component such as "dimples" which are created through the removal of material at patterned or randomised locations with specific dimensions of removal depth and diameter. Micro-grooves in the form of linear parallel, cross-hatched or wavy lines are also used [13, 17]. Textured surfaces provide advantages such as the trapping of debris and this consequently reduces the aforementioned tool-chip friction effects, increases the lubricity of the tool-chip and tool-work piece interface by providing regions of lubricant storage. This can also increase the load carrying capacity of the machining component by improving stress distribution and concentration at the contact interfaces [17].

Hence, this study aims at investigating the application of PLM as an alternative to conventional abrasive techniques in the fabrication of textured Si_3N_4 tool inserts for tribological applications like the machining of cast iron and related alloys. The specimen under consideration is a Si_3N_4-SiC composite ceramic, doped with Al_2O_3 and yttrium oxide (Y_2O_3) as densification agents during pressure sintering. The surface texturing method applied was the micro-grooving of parallel lines onto the insert surfaces. This study considered the following objectives: (i) profiling of the resulting material removal rates achieved under varied processing parameters in order to obtain a material removal depth not higher than 10µm (keeping in mind the design specifications (thickness) of the tool insert), (ii) analysing the resulting surface roughness along the micro-grooves to determine if the profiles fit the criteria of a two-dimensional (2D) mean surface roughness interval of $1.5\mu m \leq Ra \leq 2.5\mu m$ and, (iii) obtaining an overall three-dimensional (3D) mean surface roughness for the fully textured surfaces within the interval $2.5\mu m \leq Sa \leq 5.0\mu m$. The morphology of the laser treated surfaces was also analysed to understand the evolution of surface

topography and surface chemistry upon laser irradiation. This paper illustrates the material response during surface texturing by PLM without the tribological behaviour of the generated surfaces.

2. MATERIALS AND METHODS

2.1 Materials and Laser System

Laser processing was carried out on the commercially available gas pressure sintered Si_3N_4-SiC ceramic (14% α- Si_3N_4, 76% β- Si_3N_4, 5% SiC, 3% Al_2O_3 and 2% Y_2O_3), supplied by CeramTec, Germany. The sample dimensions were 4.8x14x14 mm^3 and their material properties are displayed in Table 1. Surface texturing was performed using a pulsed mode, 25W Neodymium-doped yttrium aluminium garnet laser system (Q-switched, Nd: YAG, model: DML40 Deckel Maho Gildemeister manufactured by Lasertec, USA) with a wavelength of 1064nm. The laser system was equipped with Lasersoft 3D computer numerical control (CNC) to enable 3-axis (X, Y, Z) processing. The laser beam of a pulse duration of 250 ns was delivered through a series of mirrors and focused through a convex lens as shown by the schematic on Fig. 1. Laser machining was carried out by varying pulse energy (energy density), pulse overlap by changing the scanning speed alongside pulse repetition rate as shown in Table 2. The experiments were conducted under atmospheric conditions (air and room temperature) using a Gaussian spatial laser beam profile of diameter, Ø = 40µm.

2.2 Machining Methods and Analytical Tools

Prior to laser machining, the mean surface roughness (Ra) of the samples was analysed using a Confocal Laser Scanning Microscope (CLSM, Model: LEXT OLS3100, Olympus Corporation, USA). The material removal during surface texturing was conducted using both two-dimensional (2D) machining and three-dimensional (3D) machining procedures adopted from the work by Samant [1] and Vora et al [3, 5, 26].

2.2.1 Two-dimensional (2D) laser machining

Three evenly spaced (1.5mm) single pass laser scans were created on the samples for each parameter combination to reduce the level of uncertainty and minimize the effect of debris on the characterisation outputs (removal depth, Z and laser scan width, W). Pulse repetition rate (f) was varied alongside scanning speed (v) to investigate the effect of lateral pulse overlap (OV_x) on material removal as illustrated on Fig.2. The lateral pulse

overlap, number of pulses delivered and the average energy density were estimated using the Eqs. (1, 2, 4) respectively as shown in Table 2. The machined samples were then analysed using a CLSM to measure the material removal depth, laser scan width and mean surface roughness along the centre of the generated tracks. From the three single pass laser scans per parameter, five values of Ra, Z and W were collected and the average was used for analysis alongside the standard deviation. The extracted values were then used to estimate the material removal rate (MRR) per unit length as follows:

$$MRR = 0.25.\pi.Z.W.\rho \quad (5)$$

Where: ρ (kg/m^3) denotes the density of the material. The data points were then fitted into model equations determined using least square regression in order to establish the correlation between the processing outputs (Ra, Z, and W) and the laser parameters (E_p and OV_x). Due to the specifications for the tool insert thickness restricted by the final tool geometry, a ~10µm material removal depth was set as the target for the entire PLM process. Hence, this value was used as a laser parameter selection criterion for removal depth. The two-dimensional surface roughness which was measured along the laser tracks was used as a secondary selection criterion whereby the Ra values had to satisfy the interval of $1.5\mu m \leq Ra \leq 2.5\mu m$.

2.2.2 Three-dimensional (3D) laser machining

The selection of laser parameters for the fully textured surfaces first had to satisfy the criterion set for 2D machining. Due to the finite size of the beam diameter relative to the sample dimensions, a unidirectional scanning strategy was used to generate the parallel micro-grooves on sample surfaces. This machining strategy allowed the laser beam to move beyond the sample length (14mm) by completing 15mm scan in the x-direction while the subsequent laser scan began 20 µm away in the y-direction next to the previous scan as shown on Fig. 3.

The shift in the y-direction (S, scan spacing) as illustrated in Fig. 2, allowed for a gradual increase in the number of scans (P) for complete surface coverage. Moreover, the scan spacing determined the transverse pulse overlap or overlap in the "y" direction (OV_y = 50%) which was calculated as in Eq. 2 in Table 2 and was kept constant during 3D machining. The fully textured samples were then analysed using the CLSM for the overall 3D surface roughness. The selection criterion specified for the fully textured surfaces was the mean roughness interval of $2.5\mu m \leq Sa \leq 5.0\mu m$. In addition, the scanning electron microscope (SEM) (JSM-7001F, JEOL, Japan) equipped

with energy-dispersive x-ray (EDX) detectors was used to observe the surface morphology and quantify the induced changes in the chemistry of the fully textured surfaces.

3. RESULTS AND DISCUSSION

3.1 Material Removal

The Figs. 4-7 depict the results of the material behavior during PLM at varied laser pulse energy (0.1-0.6mJ or 0.8-4.8x10^5 J/m^2) and lateral pulse overlap (OV_x=50, 75 and 88%) during 2D machining. On Figs. 4-5, it can be observed that the material removal depth and scan width of machined tracks generally increased with an increase in laser pulse energy and lateral overlap. This trend was as a result of the excitation of the majority of the surface atoms after absorbing laser energy which was above the materials ablation threshold. As shown on Fig. 6a, there was no significant material removal observed when energy of 0.1mJ pulse (0.80x10^5 J/m^2) was used. These results show that the minimum energy required to induce surface damage for the SL506-Si_3N_4 ceramic (material removal threshold) is within this energy range. Above the pulse energy of 0.1mJ, it can be inferred that the majority of the irradiated atoms were evolved from the surface by evaporation as result of the surface temperatures that exceeded the evaporation or sublimation point (2173-3600K) [1-4]. As a result, a cavity was created on the machined surface and quantified using removal depth and scan width as shown on Figs. 4-6.

In line with the targeted removal depth of 10µm, the results show that this value was achieved within a pulse energy range 0.15-0.30mJ (1.19-2.38x10^5 J/m^2). The actual co-ordinates for the intersection of the removal depth line and lateral pulse overlap curves can be observed at parameter combinations of pulse energy and lateral overlap (E_p: OV_x) of [0.15mJ (1.19x10^5 J/m^2): 88%], [0.20mJ (1.59x10^5 J/m^2); 75%) and [0.30mJ (2.38x10^5 J/m^2); 50%). On Fig. 5, it is also shown that with an increase in pulse energy, the values of the laser scan width approached the range of 80-90µm which is more than double the average beam diameter of 40µm. However, the effect of pulse overlap became less significant at higher pulse energies around 0.44-0.60 mJ (3.50-4.77x10^5 J/m^2) where an average maximum laser scan width of ~90 µm was obtained. The observed surface response can be due to the fact that the beam diameter was kept constant (Ø=40µm) and this causes the region in the beam profile at which the laser energy density is above the material removal threshold to remain constant. Hence, a consequential plateau of the diameter of the irradiated zone is reached regardless of an increase in the number of pulse delivered on single spot. These results are congruent with findings presented by Dunn et al [16].

However, the opposite was observed on the material removal depth values as they increased with an increase in lateral pulse overlap as highlighted earlier. These results are in agreement with the findings reported by Vora et al [3, 5] where it was shown that when the number of pulses delivered on a single spot is increased (for 50, 75, 88%, N=2, 4, and 8 respectively), the surface temperature history induced by the first pulse is gradually elevated by subsequent pulses due to heat accumulation. If the energy delivered by the first pulse is sufficient to induce melting, the repeated deposition of energy causes the material to remain in the liquid state for a prolonged period of time, thus leading to a continuous surface deformation and even material removal by evaporation if the surface temperatures reach above the evaporation temperatures. The subsequent increase in crater depth was attributed to an increase in recoil pressure which is a downward load exerted onto the molten material by the condensing vapors as they return back to the surface due to gravity.

This causes the molten material to be pushed outwards and thus increasing the material removal depth as evidenced on Fig. 4. A detailed account of the observed surface morphology is presented in Section 3.3. To predict the values of laser scan width and material removal rate at these chosen machining parameters, the data was fitted into the logarithmic equations as determined using least square regression. The fitting curves for the process, removal depth (Z, µm) and laser track width (W, µm) are as follows:

$$Z = a.\exp(b.OV_x).\ln(E_p) + c.\exp(d.OV_x) \quad (6)$$

$$W = g.\exp(h.OV_x).\ln(E_p) + m.\exp(p.OV_x) \quad (7)$$

Where: a, b, c, d, g, h, m and p are the fitting curve coefficients, Ep (mJ) and OV_x (%) are the pulse energy and lateral overlap respectively. The values of the fitting curve constants are displayed on Table 3. The predicted removal depth and laser scan width values were then substituted into the Eq. 5 to calculate the material removal rate depicted on Fig.7. The plots followed a similar logarithmic trend exhibited on Figs. 4-5 whereby material removal rate (MRR) is a function of both laser pulse energy and lateral overlap for the selected processing parameters. From the fitting curves on Fig.5, the corresponding scan width values for the parameter combinations that produced that required material removal depth of 10µm which are E_p: OV_x = (0.15mJ; 88%), (0.20mJ; 75%) and (0.30mJ; 50%) are 76.5µm,75.5µm and 76.3µm respectively. From Fig.7, the corresponding MRR values were estimated to be 2.4mg/m, 2.2mg/m and 2.15mg/m respectively. Thus, the results show that the generated parallel micro-grooves of a

10µm depth will had an average scan width of 76.10±0.529µm which lead to an average material removal rate of 2.250±0.132mg/m as a function of the aforementioned laser parameters.

3.2 Surface Roughness Analysis

3.2.1 Two-dimensional (2D) laser machining

On the generated laser tracks, surface roughness was measured at 5 random regions along the center of the laser track to determine the average quality of the micro-grooves produced by each laser parameter. The results for the 2D mean surface roughness (Ra) as a function of pulse energy and lateral overlap are displayed on Fig.8. It can be seen that, at pulse overlaps of 50% and 75%, no significant change in Ra values was observed at lower pulse energy (0.1- 0.2 mJ) where values were within a range of Ra=1.80±0.51µm. Hence, within the near energy threshold range of the material, pulse overlap did not have a significant influence of the surface roughness profile of the laser tracks. However, when pulse energy was above 0.2mJ, Ra values of the respective curves increased except for those of the 50% overlap.

The Ra values for the 50% lateral overlap plot remained within a mean of Ra=1.6±0.45µm while a moderate increase was observable for the 75% overlap from Ra=1.80±0.92µm at 0.2mJ ($1.59x10^5$ J/m^2) to maximums of 2.25±0.12µm at 0.6mJ ($4.77x10^5$ J/m^2). When considering the 88% pulse overlap, the results showed a linear increase in roughness values from an average of Ra=1.80±0.42µm at 0.2mJ to maximums of 4.75±0.58µm at 0.60mJ. This increase can be attributed to the reasons highlighted in Section 3.1. Also, the micro-pores created on the sample surface shown on Fig. 10(e) which were formed on the surface as the pulse energy was increased can also contribute to an increase in surface roughness. Compared to the surface as-received with roughness interval of Ra=0.53±0.422µm, the results show that the PLM process increased the surface roughness in all the laser parameters investigated. When considering the process objective regarding target surface roughness of Ra ϵ[1.5,2.5µm], the results show that this condition was satisfied at all lateral pulse overlaps when a pulse energy range of E_p ϵ [0.10,0.30 mJ] or average energy density of F ϵ [$0.80x10^5$ J/m^2, $2.38x10^5$ J/m^2] was used.

3.2.2 Three-dimensional (3D) laser machining

For 3D machining (or full surface texturing), four combinations of processing parameters within the mentioned pulse energy interval were selected to accommodate the near and above threshold laser energy settings. These included combinations of 0.1mJ and 0.3mJ with 50% and 88% lateral pulse overlap as shown on Fig. 9. These settings were also selected so as to provide insight on the microstructural evolution of the material surfaces when the gentle and intense material removal was induced. The Fig. 9 shows that all surfaces were successfully machined using the selected parameters. However, the differences in the quality of the parallel micro-grooves indicated that each processing parameter induced a unique surface morphology upon laser impact. On Fig. 9(a), it can be seen that at low pulse energy (0.1mJ, $0.80 \times 10^5 J/cm^2$), the linear micro-groves were not successfully generated as exhibited by the low intensity of the laser tracks.

As shown on Fig. 9(b), an increase in lateral pulse overlap to 88% did not produce the intended texture as evidenced by the poor distinction between the laser tracks. Although the surface roughness increased from Sa = 1.85±0.09µm to Sa = 2.13±0.12µm which was slightly below the desired limits of $2.5\mu m \leq Sa \leq 5.0\mu m$, this was considered as an unsatisfactory outcome. The surfaces textured using the above threshold laser energy settings (0.3mJ, 2.38×10^5 J/m^2) for material removal and varied lateral pulse overlap are exhibited on Figs. 9(c-d). The results showed an improvement in the quality of the surface texture at 50% lateral overlap whereas an increase to 88% created a distorted texture with no clear separation between the micro-grooves. In addition, the surface roughness was increased by an increase in pulse energy and lateral overlap from Sa = 4.03±0.27µm to Sa = 24.95±0.81µm.

These findings were considered as a positive outcome since the surface roughness of the generated profiles was within the desired limits. From these results, it can be deduced that the control of the surface texture parameters (roughness and material removal) was achievable at lower lateral pulse overlap. In this way, the effects of heat accumulation were be minimized even when pulse energy is increased.

3.3 Surface Morphology and Chemistry

As a thermally based machining process, the material removal during PLM occurs a result of numerous physical mechanisms which are dictated by the duration or width of the laser pulse. Since the utilized laser system

delivered longer pulses (250ns), based on the research by various scholars, material removal was expected to occur by melting, dissociation and evaporation due to longer laser-material interaction time [16, 22, 23]. This assumption was confirmed by the microstructures depicted on Fig. 10, which show the residual surface deformation as a result of PLM.

In addition, various researchers [2, 25-26] demonstrated that the processing conditions (temperature, pressure, and surrounding atmospheric gases) can also be used to influence the residual properties of the surface. The machining environment can be used to promote reactions of any form (oxidation or gas forming) with the activated surface elements or be designed to be chemically inert in order to preserve the formed surface constituents during surface deformation. From the SEM and EDX results presented in Fig. 10, it is shown the PLM process which was carried out in air, did not only influence the residual surface topography but a significant change in the surface chemistry was induced as well.

The effect of the changes in microstructure and chemistry on the functionality of the processed components was however not evaluated as this was beyond the scope of this work. Nonetheless, these observations will provide insight for future studies. With regards to the changes in surface chemistry, the proposed equations that describe the physical mechanisms that occurred on the surface of Si_3N_4-SiC samples are summarized in Table 4. When refering to the as-received samples displayed on Fig. 10(a-b), it can be observed that the samples had a high surface nitrogen (N, 54.10%), followed by silicon (Si, 19.74%), oxygen (O, 12.97%), carbon (10.41%) and lastly, aluminium (Al, 2.79%) by mass. The microstructures and corresponding EDX results for the surfaces that were treated using of the near threshold pulse energy are represented in Fig. 10(c-d) and 10(g-h).

The irradiated surface showed evidence of re-solidification after laser irradiation and this shows evidence of melting which generally occurs in the form of Eqs. 8-10. The equations describe the dissociation Si_3N_4, SiC and Al_2O_3 into their constituents. The decomposition of Si_3N_4 and SiC contributes to the increase in surface Si (43.39-52.02%) and Al (3.02-3.36%). Moreover, a significant loss of N (7.39-11.00%) also substantiates the dissociation reaciton which assumes this reduction by the evolution of this gas into the atmosphere.

Since all machining was conducted under atmospheric conditions (air), the solid C which originates from the decomposition and oxidation (at low temperatures) of SiC additive reacted with the oxygen from the atmosphere

to form carbon dioxide gas (CO_2) which was then lost to the atmosphere as represented in Eqs. 15-16. As a result, the C content of the surface was resduced (6.62-8.25%). It is also shown that there was a significant increase in surface O (27.79-39.24%) due to PLM. The Eqs 11-15 show that the oxidation of Si_3N_4 and SiC may have formed vapours of silicon oxide (SiO) which were later oxidised into solid silicon dioxide (SiO_2) by the atmosphere.

The SiO_2 was then re-deposited onto the surface in the form of fine particulates (debris) which as a result increased the O content of the surface as shown on Fig. 10(d, f, h, j). According to Tian et al [25], the surface SiO_2 can also react with the residual Al_2O_3 to form mullite particles (Al_2O_3. SiO_2) (Eq. 13). It is important to note that the evidence of the re-solidification was not considered as good result since the surface also presented microcracks shown on Figs. 10(c) and 10(g). According to Vora et al [3], the presence of the lateral (OV_x) and transverse overlap (OV_y) increases the number of pulse per laser spot which increases the induced thermal stresses. As a result of the thermal expansion difference between the laser interaction region and the surrounding bulk material, microcracks are then nucleated.

The presence of microcracks on the surface may compromise the performance of the tool during machining, hence this was considered undesirable on the textured surfaces. As also highlighted Section 3.3.2, the parameter combination 0.1mJ and 50-88% lateral produce the desired texture as shown on Fig. 9(a-b). Evidence presented on Fig. 10(b, g) show that the distortion in poor micro-grooves observed were due to the fact the delivered laser energy was insfuccient for material removal by evaporation but surface melting was induced instead. Thus it can be deduced that the parameters that are near the material removal threshold (~ $0.80x10^5$ J/m^2) were not suitable for producing the desired texture.

The results for the surfaces that were machined at a laser enrergy above the materials threshold (0.3mJ, $2.38x10^5$ J/m^2) are shown on Figs. 10(e-f) and 10(i-j). The EDS analysis shows a similar trend observed on the surfaces that were treated with 0.1mJ. However, the microstructures do not show evidence of melting on the surface but rather, an abundance of fine particulates re-deposited on the sample surfaces. This shows that this parameter combination (Ep=0.3mJ, OVx=50-88%) was sufficent to promote the evaporation of the generated molten material. However, the surfaces textured showed evidence of micropores at 50% lateral pulse overlap. According to Hampshire [21], the presence of mixed oxide additives (Al_2O_3 + Y_2O_3) in the cermic matrix leads to the modification of the grain boundaries into glassy phases of Y-Si-Al-O-N. It is thus hypothesised that the formation of

micro-pores on the textured surfaces may be due to the deformation (melting and evaporation) of the grain boundaries due to the high surface temperatures induced by the high laser energy density as in the Eq. 17-19. This subject is still up for further investigation in future works.

4. CONCLUSION

The surface texturing of the SL506-Si_3N_4 composite doped with SiC, Al_2O_3 and Y_2O_3 was conducted for the fabrication of machining tools using a stepwise approach consisting of 2D and 3D PLM machining procedures in a nanosecond Nd: YAG pulsed laser system. The effects of laser operating parameters such as pulse energy (energy density) and lateral and transverse pulse overlap on material removal, microstructural evolution and surface chemistry were studied. The results showed that:

- The material removal threshold of the Si_3N_4 composite in consideration was around 0.1 mJ ($0.80x10^5 J/cm^2$) for a Gaussian profile laser beam of 40 µm, pulse duration of 250 ns and at a wavelength of 1064 nm.
- During 2D machining, laser energy and pulse overlap increased material removal by a logarithmic relationship.
- An increase in the 2D roughness (Ra) values was observed at higher lateral pulse overlaps when pulse energy was increased while at intermediate and low lateral pulse overlaps, the change was minimal.
- Optimum roughness ($1.5µm \leq Ra \leq 2.5µm$) and material removal depth (10µm) were attained at a pulse energy interval of 0.1-0.3mJ ($0.80\text{-}2.38x10^5$ J/m^2) for all investigated lateral pulse overlap.
- For 3D machining (full surface texturing by parallel linear micro-grooving), the texture that satisfied both the roughness criterion ($2.5µm \leq Sa \leq 5.0µm$) and micro-groove quality was obtained at 0.3mJ ($2.83x10^5$ J/m^2).
- The surface texturing process by PLM was found to occur by dissociation and melting when the near threshold laser energy was used whereas evaporation dominated material removal at higher laser energy densities.
- The microstructural evolution and changes in surface chemistry were attributed to dissociative reactions of the ceramics major constituents and oxidative reactions induced by the machining environment.

REFERENCES

[1] A. Samant, Laser machining of structural ceramic: computational and experimental analysis: PhD diss., University of Tennessee, Knoxville, USA, 2009.

[2] P.P. Shukla, J. Lawrence, Surface characterization and compositional evaluation of a fibre processed silicon nitride (Si_3N_4) engineering ceramic, Lasers in Engineering, 20(5-6),2010, 359-370.

[3] H.D. Vora, Intergrated computational and experimental approach to control physical texture during laser machining of structural ceramics: PhD diss, University of North Texas, Texas, USA, 2013.

[4] P.P Shulka and J. Lawrance, Viability and characterization of laser surface treatment of engineering ceramics: PhD Thesis, Loughborough University, UK, 2011.

[5] H.D. Vora, N.B. Dahotre, Surface topography in three-dimensional laser machining of structural alumina, Journal of Manufacturing Processes, 19(1), 49-58, 2015.

[6] M.A. Moncayo, S. Santhanakrishnan, H.D. Vora, R.P. Paital, N.B. Dahotre, Laser surface modification of alumina: Integrated computational and experimental analysis, Ceramics International 39(6), 2013, 6207-6213, DOI: 10.1016/j.cermint.2013.01.040.

[7] D. T. Pham, S. S. Dimov and P. V. Petkov, Laser milling of ceramic components, International Journal of MAchine Tools & Manufacture, 47(3-4), 618 - 626, 2007.

[8] S. Hampshire, Silicon nitride ceramics – review of structure, processing and properties. Journal of Achievements in Materials and Manufacturing Engineering, 24(1), 2007, 43-50.

[9] C-J. Lee, C-J., H-C. Liu, H-H. Lu, T. Goto, R Tu., C-A. Wang, S. Pavol, J-L. Ruan, P.K. Nayak, J-H. Chen, Q-Y. Chen, J-L. Huang, Indentation deformation and microcracking in β-Si_3N_4-based nanoceramic. Journal of American Ceramic Society, 95(4), 2012, 1421-1428. DOI: 10.1111/j.1551-2916.2012.05080.x

[10] S.B. Dhage, P. Sarkar, A. D. Jayal, Investigation of surface textured cutting tools for sustainable machining, 5th International & 26th All India Manufacturing Technology, Design and Research Conference (AIMTDR 2014) December 12th -14th , 2014, Guwahati, Assam, India.

[11] F. Rabiei, A.R. Rahimi, M.J. Hadad, M. Ashrafijou, Performance improvement of minimum quantity lubrication (MQL) technique in surface grinding by modeling and optimization, Journal of Cleaner Production, 86 (1), 2015, 447-460, DOI:10.1016/j.jclepro.2014.08.045.

[12] D. Carou, E.M. Rubio, C.H. Lauro, J.P. Davim, Experimental investigation on surface finish during intermittent turning of UNS M11917 magnesium alloy under dry and near dry machining conditions, Measurement, 56(1), 2014, 136-154, DOI:10.1016/j.measurement.2014.06.020.

[13] Y. Xing, J. Deng, K. Zhang, X. Wang, Y. Lian, Y. Zhou, Fabrication and dry cutting performance of Si3N4/TiC ceramic tools reinforced with the PVD WS2/Zr soft-coating, Ceramics International, 41(8), 2015, 10261-10271, DOI: 10.1016/j.ceramint.2015.04.153.

[14] H. L. Costa and I. M. Hutchings, Some innovative surface texturing techniques for tribological purposes, Engineering Tribology, 0(0),1-20, 2014.

[15] X. Zhang, J. Deng, Y. Xing, S. Li, H. Gao, Effect of microscale texture on cutting performance of WC/Co-based TiAlN coated tools under different lubrication conditions, Applied Surface Science, 326(1), 2015, 107-118, DOI: 10.1016/j.apsusc.2014.11.059.

[16] T. Enomoto (2), T. Sugihara, S. Yukinaga, K. Hirose, U. Satake, Highly wear-resistant cutting tools with textured surfaces in steel cutting, CRIP Annals-Manufacturing Technology, 61(1), 2012, 571-574.

[17] Y. Xing, J. Deng, X. Feng, S. Yu, Effect of surface texturing on Si_3N_4/TiC ceramic sliding against steel under dry friction, Materials and Design, 52(1), 2013, 234-245, DOI:10.1016/j.matdes.2013.05.077.

[18] A. Dunn, J.V. Carstensen, K.L. Wlodarczyk, E.B. Hansen, J. Gabzdyl, P.M. Harrison, J.D. Shephard, D.P.Hand, Nanosecond laser texturing for high friction applications, Optics and Lasers in Engineering, 64(1), 2014, 9-16, DOI:10.1016/j.optlseng.2014.05.003.

[19] R. K. Singh and J. M. Fitz-Gerald, Laser induced formation of microrough structures, Nuclear Instruments and Methods in Physics Research B, 121(1-4), 363 - 366, 1997.

[20] J. H. Zhang, T. C. Lee, X. Ai and W. S. Lau, Investigation of the surface integrity of laser-cut ceramic, Journal of Materials Processing Technology, 57(3-4), 304 - 310, 1996.

[21] X. Zhu and Y. Sakka, Textured silicon nitride: processing and anisotropic properties, Sci. Technol. Adv. Mater, 9(1), 1-47, 2008.

[22] M. R. H. Knowles, G. Rutterford, D. Karnakis, A. Ferguson, Micro-machining of metals, ceramics and polymers using nanosecond lasers, International Journal of Advanced Manufacturing Technology, 33(1), 2007, 95-102. DOI: 10.1007/s00170-007-0967-2.

[23] M. S. Amer, M. A. El-Ashry, L. R. Dosser, K. E. Hix, J. F. Maguire, B. Irwin, Femtosecond versus nanosecond laser machining: comparison of induced stresses and structural changes in silicon wafers, Applied Surface Science, 242(1-2), 2005, 162-167. DOI: 10.1016/j.apsusc.2004.08.029.

[24] I. Shigematsu, K. Kanayama, A. Tsuge, M. Nakamura, Analysis of constituents with laser machining of Si_3N_4 and SiC, Journal of Materials Science Letters, 17(1), 1998, 737-739.

[25] Z. Tian, X. Duan, Z. Yang, S. Ye, D. Jia, Y. Zhou, Ablation mechanism and properties of in-situ SiAlON reinforced BN-SiO_2 ceramic composite under an oxyacetylene torch environment, Ceramics International, 40(7 Part-B), 2014, 11149-11155.

[26] Y. Ho, H.D. Vora, N.B. Dahotre, Laser surface modification of AZ3IBMg alloy for bio-wettability, Journal of Biomaterials Applications, 0(0), 2014, 1-4. DOI: 10.1177/0885328214551156.

ACKNOWLEDGEMENTS

The authors with to acknowledge the Fraunhofer Institute for Thin Films and Surface Technology (ITS) and the Council of Scientific and Industrial Research- National Laser Centre (CSIR-NLC) for initiating this project. The research funding provided by the National Research Fund (NRF) – Thuthuka Projects for funding (Ref. No. TTK20110706000020206) is also acknowledged.

Table

LIST OF TABLES

Table 1. Properties of the machined samples.

Material	Density (kg/m^3)	Colour	Expansion coefficient ($x10^{-6}$) (1/K)	Thermal conductivity (W/m. K, at 20°C)	Reflectivity
Si_3N_4-SiC (SL506)	3244	Light Green	3.92	23.6	0.15

Table 2. Range of laser processing parameters.

Parameter	Formula / Nomenclature	Units	Values	Equation Number	Formula Reference
Beam diameter	Ø	µm	40	-	-
Pulse energy	E_p	mJ	0.1, 0.15, 0.17, 0.20, 0.22, 0.30, 0.44, 0.60	-	-
Pulse width	P_w	ns	250	-	-
Pulse repetition rate	f	kHz	10, 20, 30	-	-
Laser scanning speed	v	mm/s	50, 100, 150, 200, 300, 400, 600	-	-
Laser scan spacing	S	µm	20	-	-
Lateral pulse overlap	$OV_x = 100.\left[1 - \left(\frac{v}{f.Ø}\right)\right]$	%	50, 75, 88	(1)	[1,3]
Number of pulses per corresponding lateral pulse overlap	$N = \frac{v}{f.Ø}$	-	2, 4, 8	(2)	-
Transverse pulse overlap	$OV_y = 100.\left(1 - \frac{S}{Ø}\right)$	%	50	(3)	-
Average Energy Density per corresponding pulse energy	$F = \frac{E_p}{0.25.\pi.(Ø)^2}$	$x10^5$ J/m^2	0.80, 1.19, 1.35, 1.59, 1.75, 2.38, 3.50, 4.77	(4)	[3,5]

Table 3. Coefficients for the material removal, scan width and material removal fitting curves.

Coefficient	a	b	c	d	G	h	m	p
Value	3.127	0.026	5.7998	0.0286	45.15	-0.018	105.12	0.001

Table 4. List of possible surface reactions that occur during pulsed laser machining for the SL-506-Si_3N_4 ceramic.

#	Physical Process	Chemical Equation	Reference
8	Dissociation	$Si_3N_4(s) \rightarrow 3Si(l) + 2N_2(g)$; $Si(l) \leftrightarrow Si(s)$; $Si(l) \leftrightarrow Si(g)$	[1, 2,24]
9	Dissociation	$SiC(s) \rightarrow Si(l) + C(s)$; $Si(l) \leftrightarrow Si(s)$; $Si(l) \leftrightarrow Si(g)$	[1, 24]
10	Dissociation	$Al_2O_3(s) \leftrightarrow Al_2O_3(l) \rightarrow 2Al(l) + \left(\frac{3}{2}\right)O_2(g)$	[1, 3, 24,25]
11	Oxidation	$2Si_3N_4(s) + 3O_2(g) \rightarrow 6SiO(g) + 4N_2(g)$	[1, 24]
12	Oxidation	$SiO(g) + \left(\frac{1}{2}\right)O_2(g) \rightarrow SiO_2(s) \leftrightarrow SiO_2(l) \leftrightarrow SiO_2(g)$	[2,24]
13	Solidification	$Al_2O_3(l) + SiO_2(l) \rightarrow Al_2O_3.SiO_2\ (l)$	[24-25]
14	Oxidation	$Si_3N_4(s) + \left(\frac{11}{2}\right)O_2(g) \rightarrow 3SiO(g) + 4NO_2(g)$	[2,24]
15	Oxidation	$2SiC(s) + O_2(g) \rightarrow 2SiO(g) + 2C(s)$	[24]
16	Oxidation	$2C(s) + O_2(g) \rightarrow 2CO(g)$; $2CO(g) + O_2(g) \rightarrow 2CO_2(g)$	[24]
17	Oxidation	$Y_4(Al,Si)_2(N,O)_{9-x}(s) + \left(\frac{4+x}{2}\right)O_2\ (g) \rightarrow 2SiO_2(s) + 2Y_2O_3(g) + Al_2O_3(l) + \left(\frac{9-x}{2}\right)N_2\ (g)$	-
18	Oxidation	$\alpha - Y_2(Al,Si)_3(N,O)_7(s) + \frac{19}{2}O_2\ (g) \rightarrow 3SiO_2(s) + 2Y_2O_3(g) + \frac{3}{2}Al_2O_3(s) + \frac{7}{2}N_2\ (g)$	-
19	Oxidation	$Si_2Al_3O_7N\ (s) + \frac{3}{4}O_2\ (g) \rightarrow 2SiO_2(s) + \frac{3}{2}Al_2O_3(s) + \frac{1}{2}N_2\ (g)$	[24]

Figure

Click here to download high resolution image

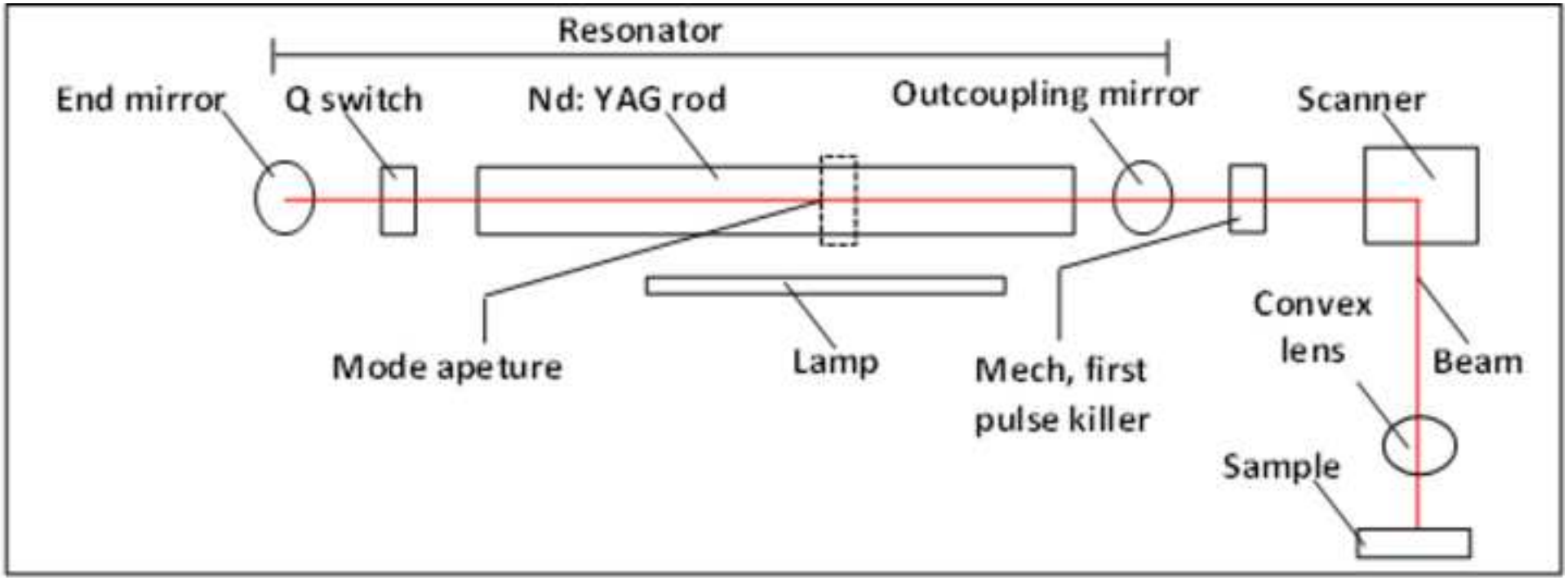

Figure

Click here to download high resolution image

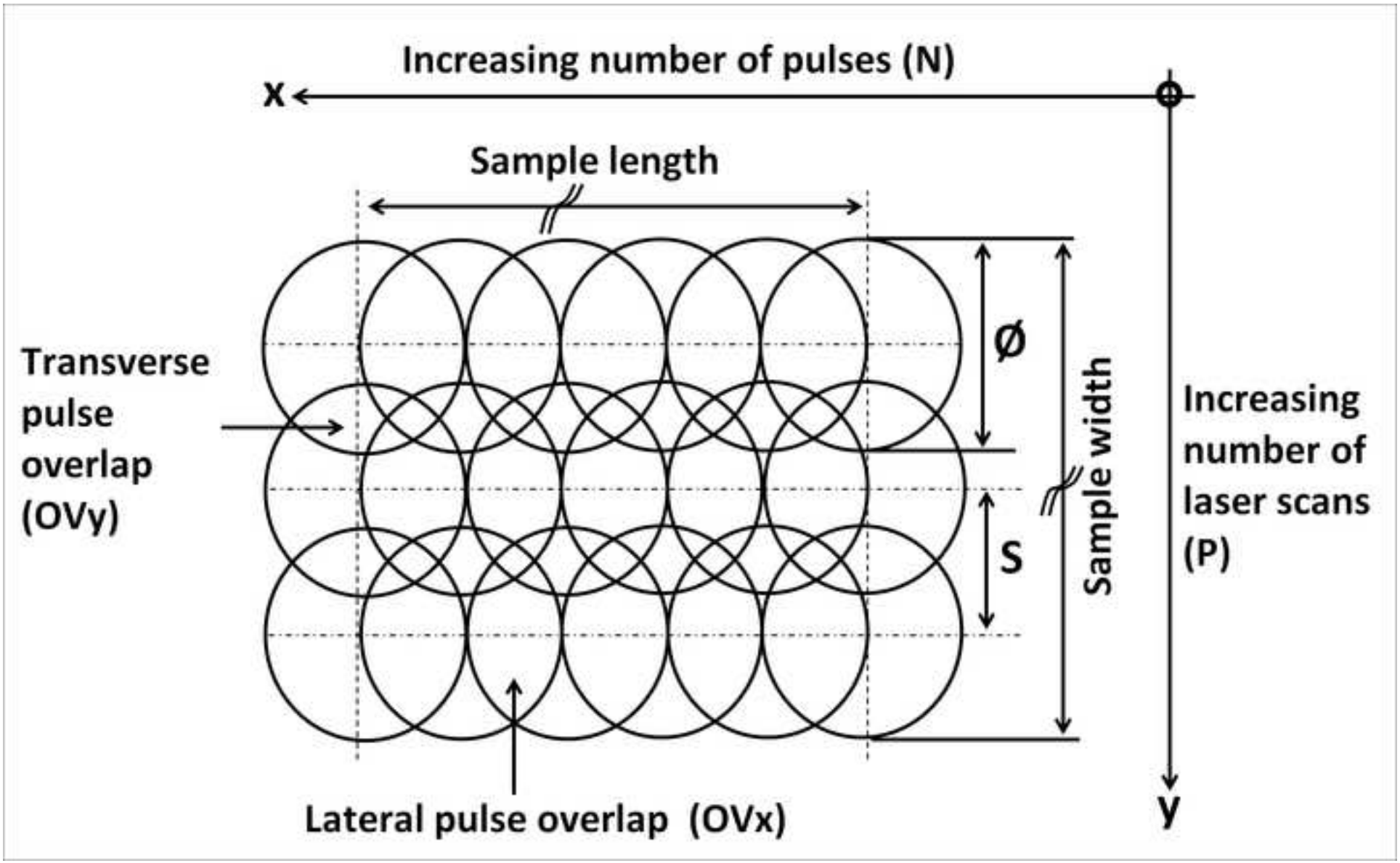

Figure

Click here to download high resolution image

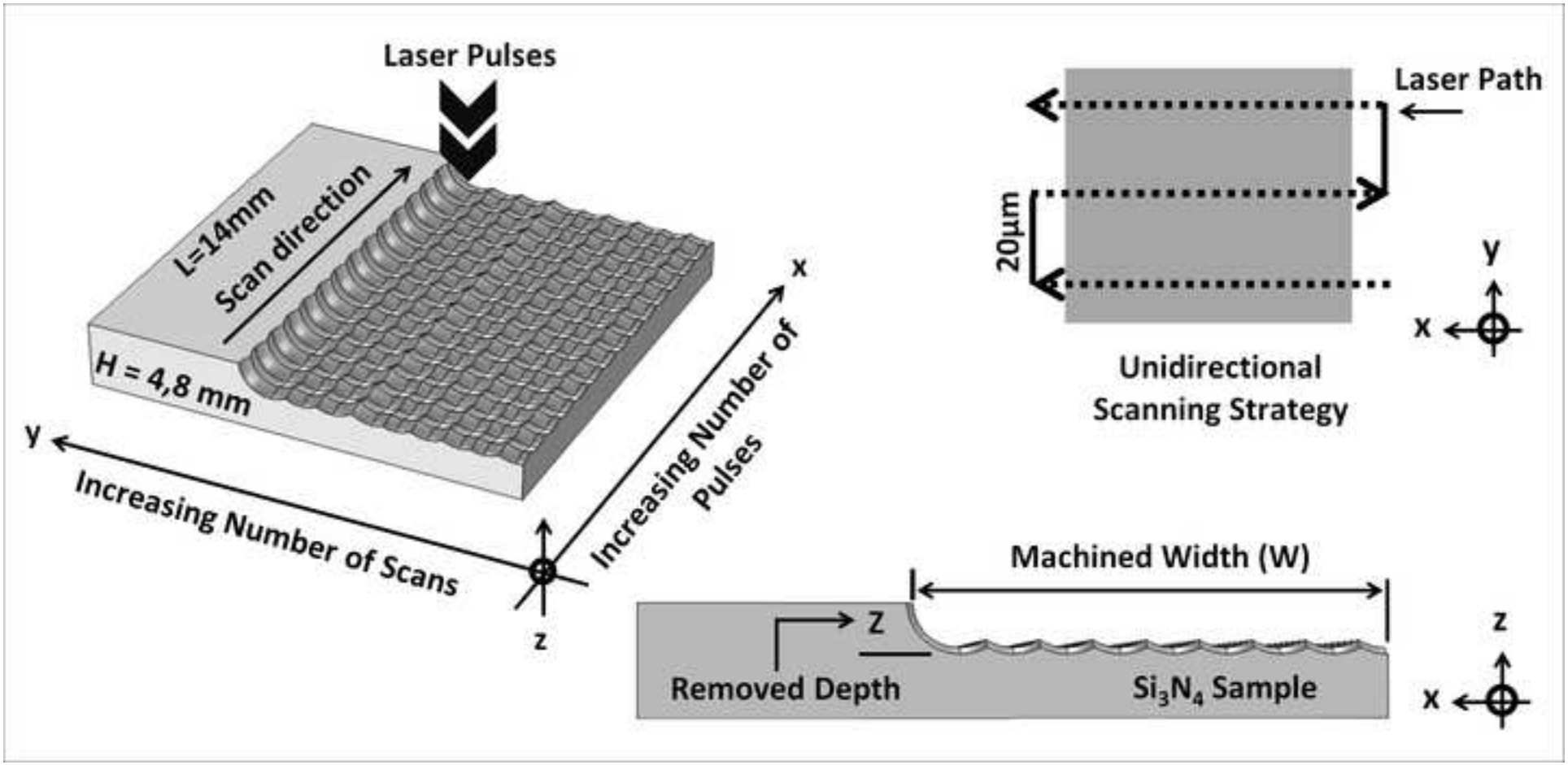

Figure

Click here to download high resolution image

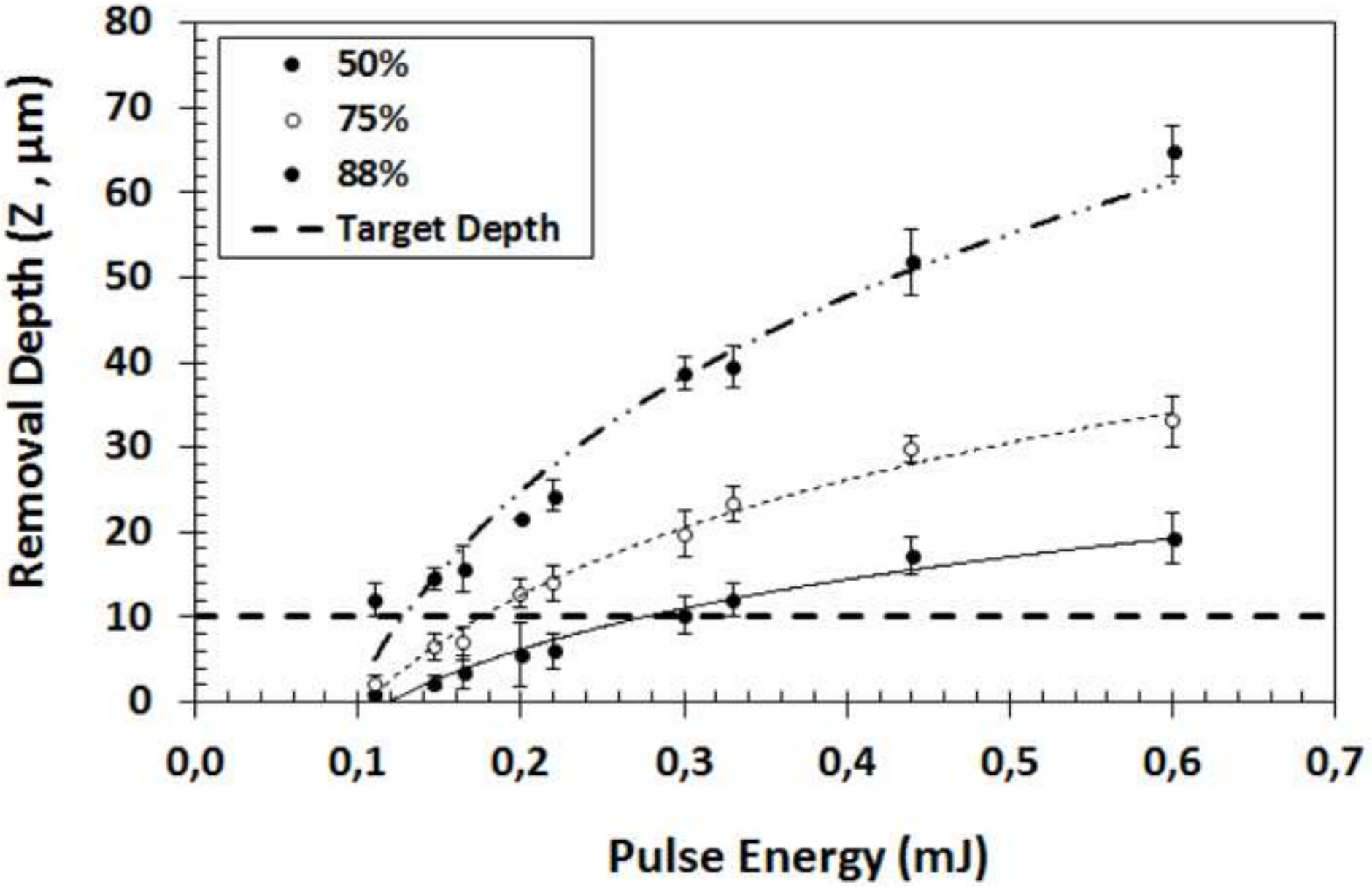

Figure

Click here to download high resolution image

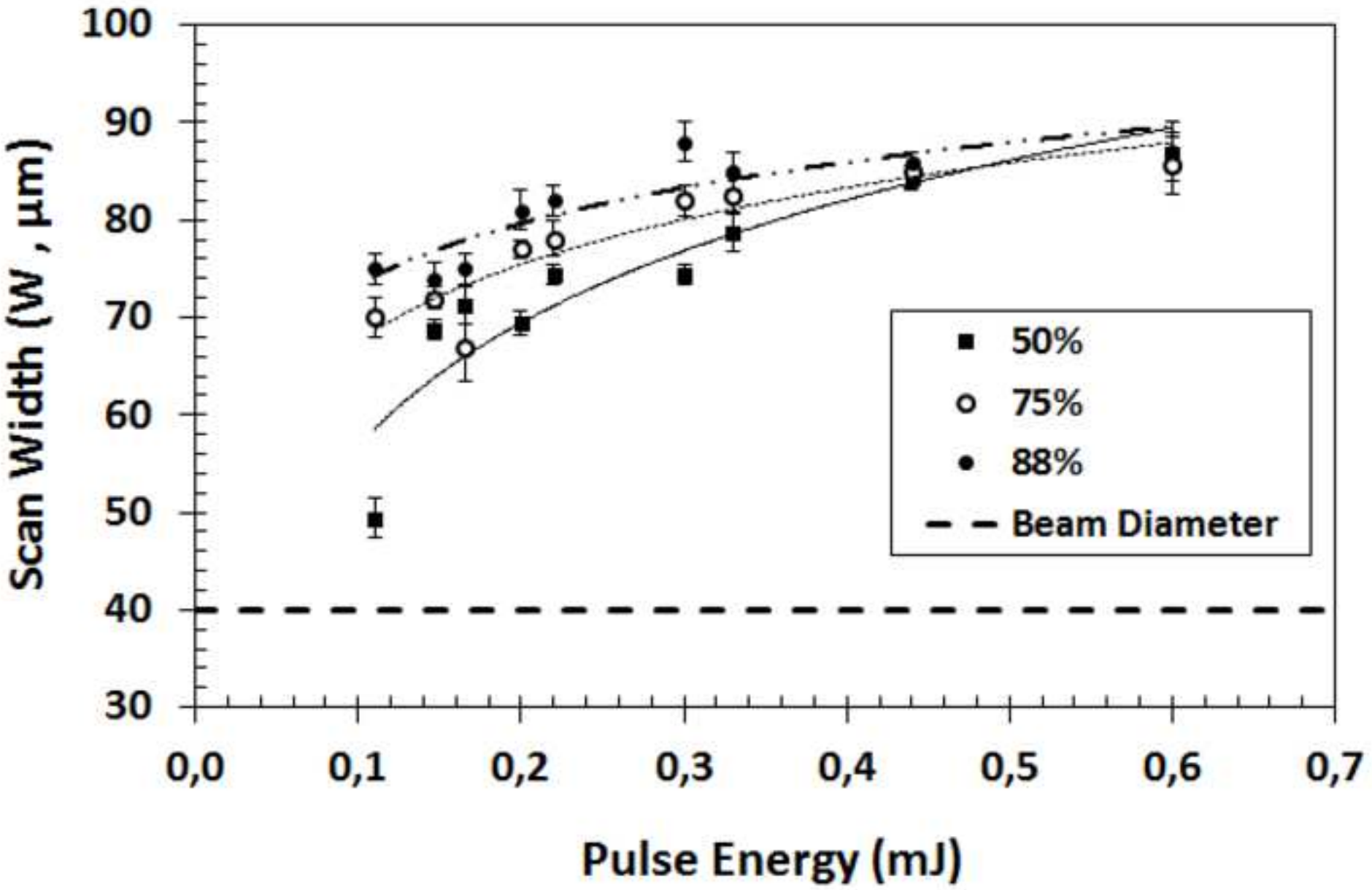

Figure
Click here to download high resolution image

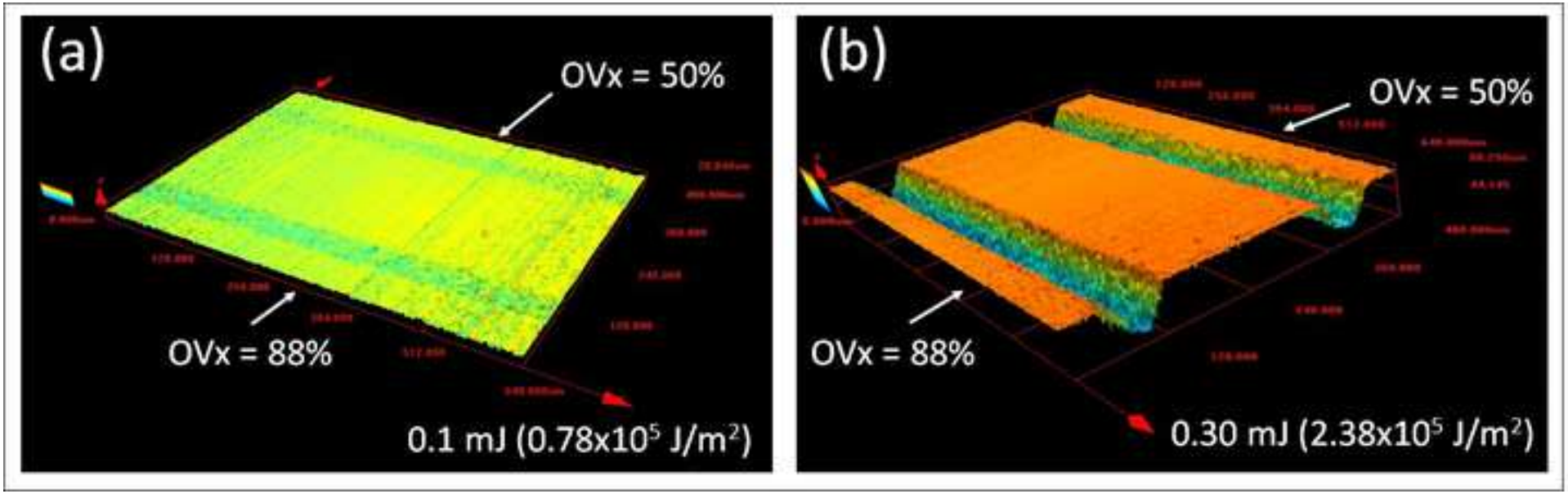

Figure
Click here to download high resolution image

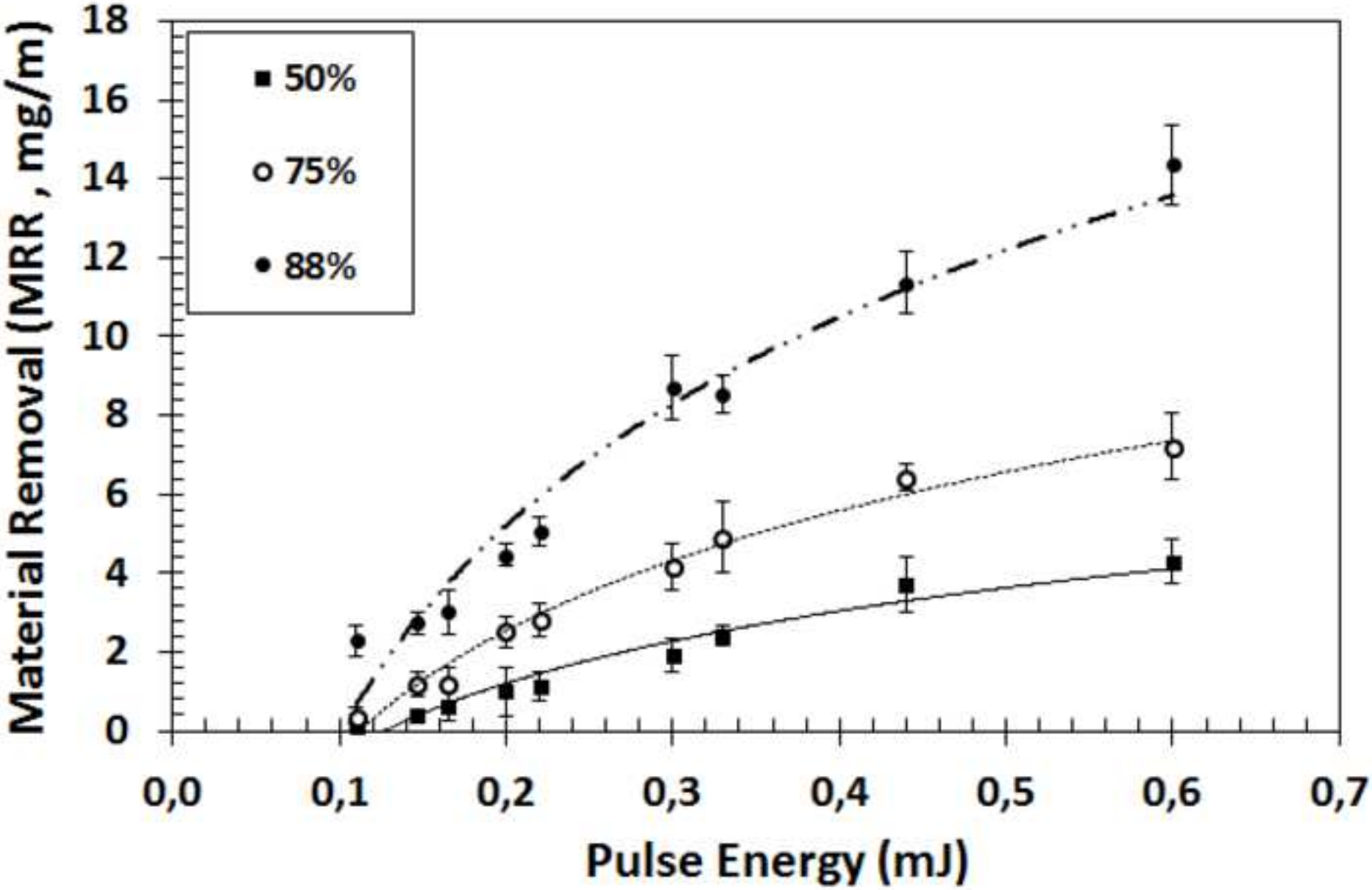

Figure
Click here to download high resolution image

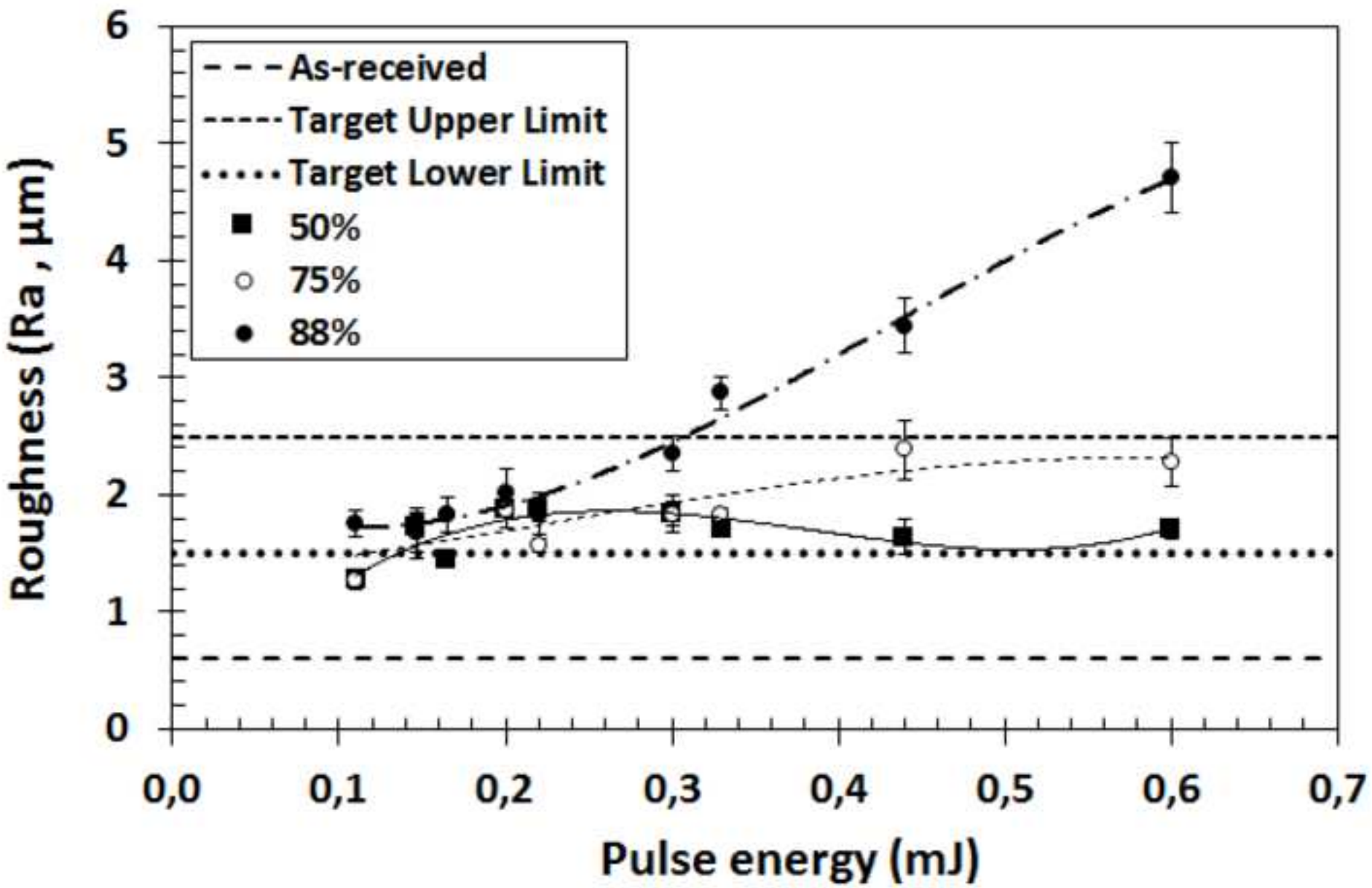

Figure
Click here to download high resolution image

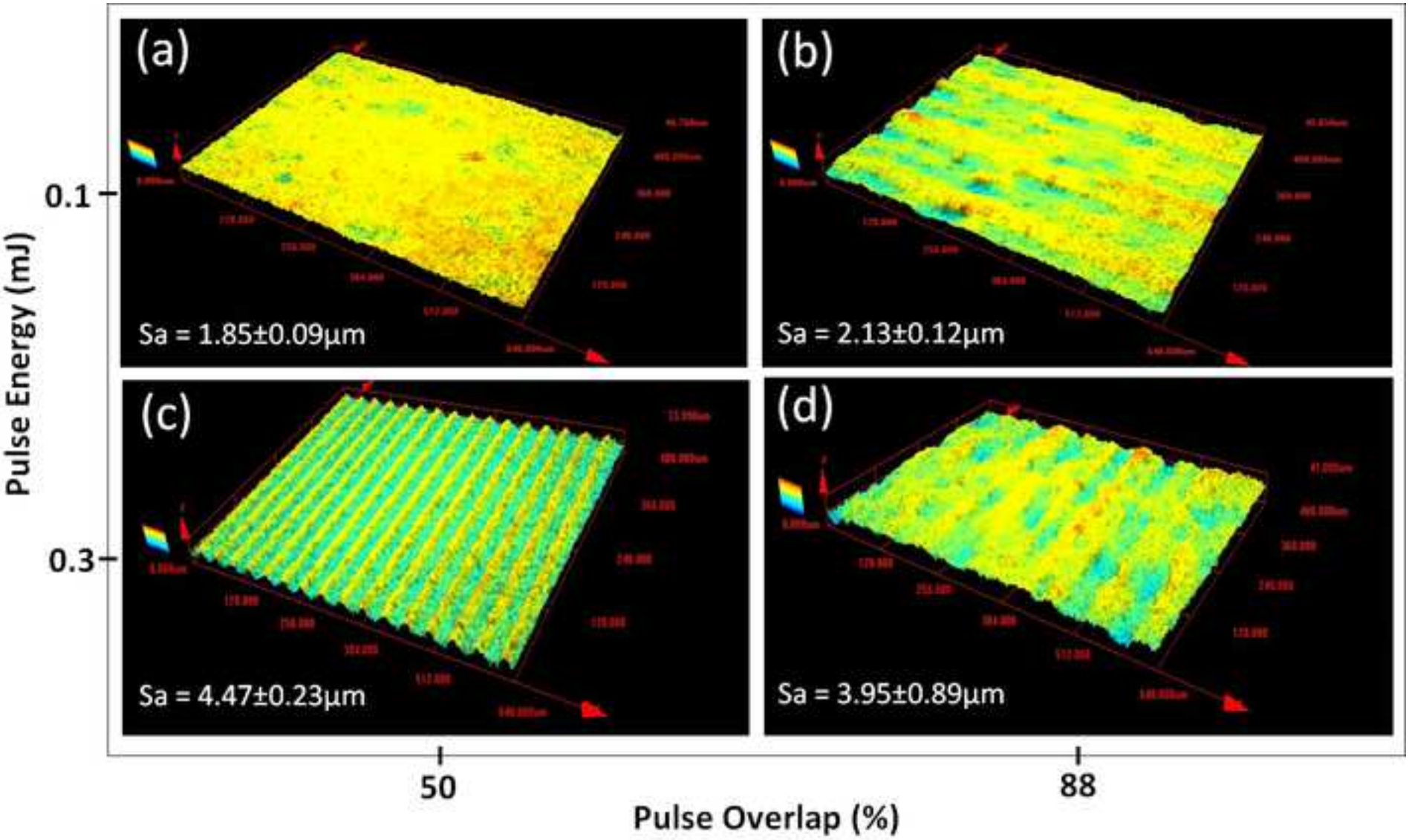

Figure

Click here to download high resolution image

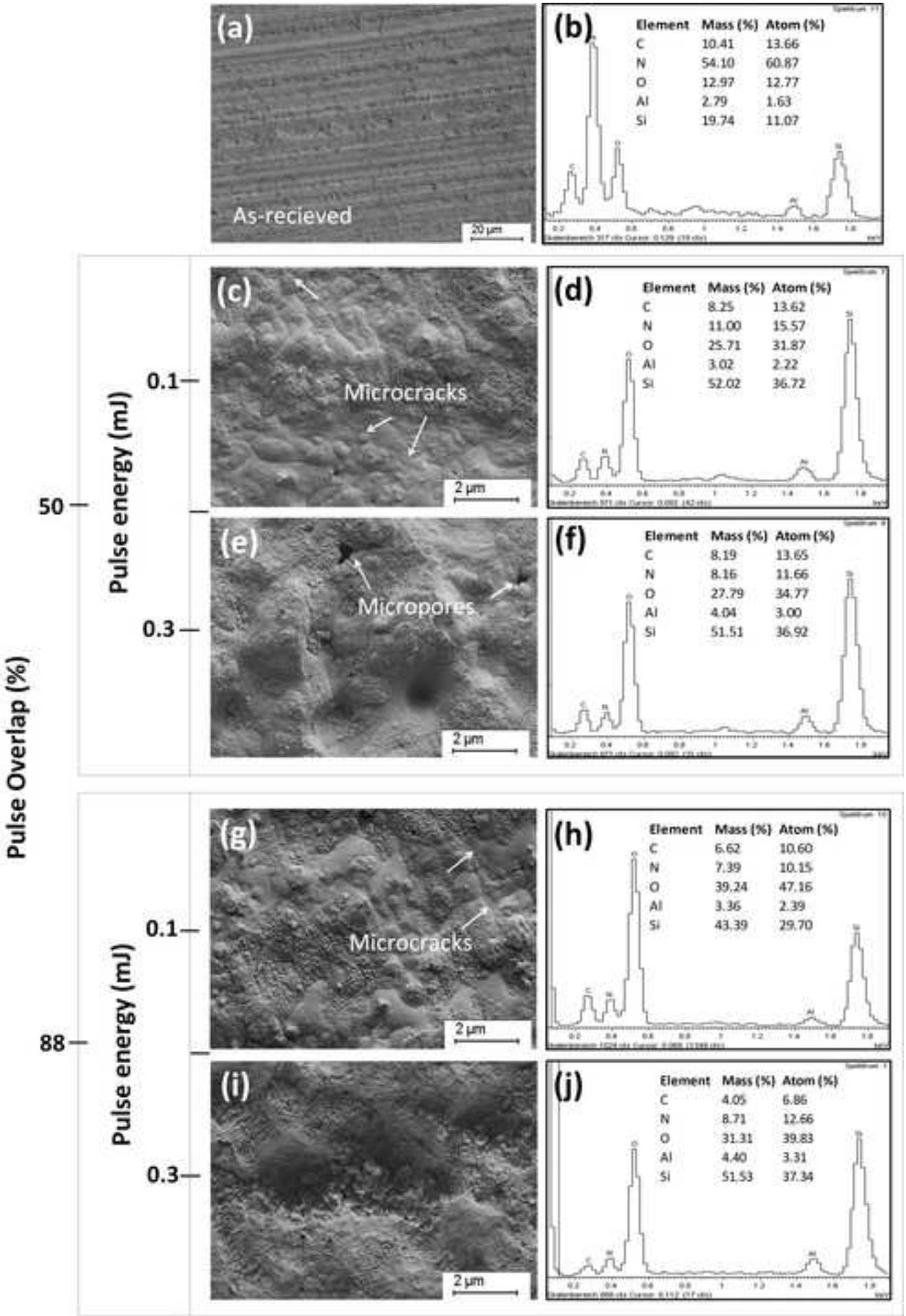

FIGURE CAPTIONS

Fig.1. Schematic of the experimental setup.

Fig.2. Schematic showing lateral and transverse pulse overlap for a unidirectional scanning strategy.

Fig.3. Illustration of the 3D machining procedure used for surface texturing, the removed depth, width and laser scanning strategy.

Fig.4. Material removal depth as a function of pulse energy and lateral overlap in relation to the targeted depth (Z=10µm).

Fig.5. Laser scan width as a function of lateral pulse overlap and energy in relation to the beam diameter (Ø=40µm).

Fig.6. Typical confocal laser scanning microscope images for the laser scans created during 2D machining using the near and above material removal threshold laser parameters.

Fig.7. Material removal rate as a function laser pulse energy and lateral overlap.

Fig.8. Mean surface roughness for the single pass laser scans created using a 2D machining procedure.

Fig.9.The CLSM three-dimensional surface morphology images of the SL506-Si_3N_4 ceramic at the near and above material removal threshold laser parameters.

Fig.10. Microstructural evolution of textured SL506-Si_3N_4 surfaces at varied laser energy and lateral pulse overlap.

Graphical Abstract

Click here to download high resolution image